ACS APPLIED MATERIALS & INTERFACES

Research Article

www.acsami.org

Solution-Processed Highly Efficient $Cu_2ZnSnSe_4$ Thin Film Solar Cells by Dissolution of Elemental Cu, Zn, Sn, and Se Powders

Yanchun Yang, Gang Wang, Wangen Zhao, Qingwen Tian, Lijian Huang, and Daocheng Pan*

State Key Laboratory of Rare Earth Resource Utilization, Changchun Institute of Applied Chemistry, Chinese Academy of Sciences, 5625 Renmin Street, Changchun, Jilin 130022, China

Supporting Information

ABSTRACT: Solution deposition approaches play an important role in reducing the manufacturing cost of $Cu_2ZnSnSe_4$ (CZTSe) thin film solar cells. Here, we present a novel precursor-based solution approach to fabricate highly efficient CZTSe solar cells. In this approach, low-cost elemental Cu, Zn, Sn, and Se powders were simultaneously dissolved in the solution of thioglycolic acid and ethanolamine, forming a homogeneous CZTSe precursor solution to deposit CZTSe nanocrystal thin films. Based on high-quality CZTSe absorber layer, pure selenide CZTSe solar cell with a photoelectric conversion efficiency of 8.02% has been achieved without antireflection coating.

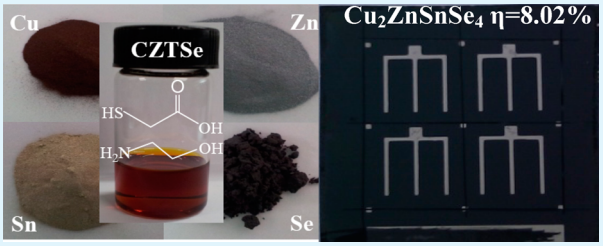

KEYWORDS: *CZTSe, thin film, solar cells, kesterite, solution process*

1. INTRODUCTION

Earth-abundant kesterite $Cu_2ZnSn(S,Se)_4$ (CZTSSe) absorbing materials have been getting significant attention in the thin film solar cells due to their suitable band gaps, high absorption coefficient, and low material cost. Different from Cu(In,Ga)-$(S,Se)_2$ (CIGSSe) thin film solar cells, solution-deposited CZTSSe solar cells exhibit much higher photoelectric conversion efficiencies (PCEs) than those fabricated by vacuum-based approaches.[1,2] Recently, CZTSSe thin film solar cells with PCEs of 8.0−12.6% have been achieved by a hydrazine-based solution approach.[3−9] In this approach, Cu_2S, S, Zn, SnSe, and Se were used as the starting materials to fabricate CZTSSe thin films. Besides, high performance CZTSSe thin film solar cells have also been respectively demonstrated by a nanocrystal-based route and a sol−gel approach, and the metal salts were usually used as their starting materials.[10−13] High efficiency solution-processed CZTSSe solar cells usually require a postselenization or a postsulfurization process, which is used to tune the band gap of CZTSSe and optimize the device performance by changing the S/Se ratio. However, due to the different volatilities of sulfur and selenium, it is very difficult to finely control the S/Se ratio in final CZTSSe thin films, which will lead to the poor batch-to-batch reproducibility since the PCEs of the CZTSSe solar cells are strongly related on the S/Se ratio.[5] Therefore, the pure sulfide CZTS and pure selenide CZTSe solar cells have recently received a great deal of attention in order to ensure better reproducibility. For the pure selenide CZTSe solar cells, the PCEs above 8% have been reported by some vacuum-based approaches,[14−16] but there are few reports about the high-efficiency solution-deposited pure selenide CZTSe solar cells in literature.[17]

Recently, Mitzi's group and Yang's group reported that a number of metal chalcogenides such as Cu_2S, In_2Se_3, SnSe, etc., can be dissolved in anhydrous hydrazine in the presence of excess selenium or sulfur.[5,6] More recently, Brutchey and co-workers found that the nine kinds of metal chalcogenides (V_2VI_3, V = As, Sb, Bi, VI = S, Se, Te) can be dissolved in the mixed 1,2-ethanedithiol and 1,2-ethylenediamine.[18] Compared to high-purity metal chalcogenides, high-purity metal powders are substantially cheaper and easy commercially available, which impels us to develop a new solution approach by using low-cost Cu, Zn, Sn, and Se powders as the starting materials to fabricate pure selenide CZTSe solar cells. According to a previous report by Zhang and co-workers, the elemental selenium can be dissolved in the mixed dodecanthiol and oleylamine.[19] Very surprisingly, except for nonmetallic Se, we found that metallic Cu, Zn, and Sn powders are also dissolved in the mixture of thioglycolic acid and ethanolamine solution despite the absence of Se (see Figure S1 in the Supporting Information). Here, we proposed and demonstrated a novel solution approach to fabricate CZTSe solar cells with a PCE of more than 8% by simultaneously dissolving elemental Cu, Zn, Sn, and Se powders.

2. MATERIAL AND METHODS

2.1. Chemicals. All reactants and reagents were commercially available and were used as received. Cu (99.99%), Zn (99.99%), Sn (99.99%), and Se (99.99%) powders as well as thioglycolic acid ($HSCH_2COOH$, 99%), ethanolamine ($HOCH_2CH_2NH_2$, AR), 2-methoxyethanol (AR), ammonium hydroxide (NH_4OH, 25%),

Received: September 21, 2014
Accepted: December 10, 2014
Published: December 10, 2014

   dx.doi.org/10.1021/am5064926 | ACS Appl. Mater. Interfaces 2015, 7, 460−464

cadmium sulfate (99%), and thiourea (99%) were purchased from Aladdin.

2.2. Preparation of CZTSe Precursor Solution. To prepare the solution, we loaded 1.7 mmol of Cu, 1.2 mmol of Zn, 1.0 mmol of Sn, 5.0 mmol of Se, 2.0 mL of thioglycolic acid, and 4.0 mL of ethanolamine in a 25 mL conical flask. The mixture was magnetically stirred on a 55 °C hot plate until the clear and wine-red CZTSe precursor solution was formed. Next, the total metal concentration was diluted to ~0.35 M by the addition of 5.0 mL of 2-methoxyethanol. Finally, the CZTSe precursor solution was centrifuged at 12 000 rpm for 5 min prior to spin-coating. Note that CZTSe precursor solution is stable in air for more than one month.

2.3. Fabrication of CZTSe Thin Film and Solar Cell Device. First, ~250 nm thick Mo was DC-sputtered on a glass slide (20 × 20 × 1.0 mm^3). Next, CZTSe precursor solution was spun at 2800 rpm for 30 s, followed by sintering on a 320 °C hot plate in nitrogen-filled glovebox ($[H_2O]$ < 1 ppm, $[O_2]$ < 1 ppm). Because of the big shrinkage during the formation of CZTSe nanocrystal thin film, this coating/sintering procedure was repeated several times to obtain the desired film thickness (~1.6 μm). Afterward, as-prepared CZTSe nanocrystal thin film was covered by a glass slide (25 × 25 × 1 mm^3) and was selenized in a graphite box containing 0.3 g of Se at 540 °C for 15 min, forming the selenized CZTSe thin films. Note that the glass slide was used to prevent the CZTSe thin film from the deposition of Se and promote the grain growth of CZTSe thin film.[20] Besides, the heating rate of the selenization is ~8.7 °C/s. CZTSe devices with the structure of glass/Mo/CZTSe/CdS/*i*-ZnO/ITO/Al were fabricated, and the detailed fabrication process has been reported in our previous papers.[21−23] CdS (60 nm), *i*-ZnO (70 nm), and ITO (200 nm) thin films were successively deposited by a chemical bath deposition approach, RF-sputtering, and DC-sputtering, respectively. Al grid electrode (~2.0 μm) was made though thermal evaporation. No antireflection coating was utilized. Finally, the CZTSe device with an active area of 0.3558 cm^2 was separated by a tungsten needle.

2.4. Characterizations. The viscosity of the solution was measured by Discovery DHR-II (TA Co., U.S.). Thermogravimetric analysis (TGA) was performed by a TGA/DSC 1 STARe of MEttler-Toledo. The thickness of the thin films was measured by a step profiler (AMBIOS, XP-100). The powder X-ray diffraction (XRD) patterns were taken with a Bruker D8 X-ray diffractometer. X-ray photoelectron spectra (XPS) were measured with VGESCALAB (VG Co., U.K.) at room temperature by using Mg Kα X-ray source ($h\nu$ = 1253.6 eV), and the binding energy was calibrated by the C 1s (284.6 eV). The scanning electron microscope (SEM) images were collected using a Hitachi S-4800. The energy dispersive X-ray spectrometry (EDS) was characterized by Bruker AXS XFlash detector 4010 built on the Hitachi S-4800. The Raman spectra were measured by a Renishaw inVia Raman Microscope using an excitation laser with a wavelength of 532 nm. Photocurrent density−voltage curves were recorded under the standard AM1.5 illumination (100 $mW{\cdot}cm^{-2}$) with a Keithley 2400 source meter. The external quantum efficiency (EQE) spectrum was measured by a Zolix SCS100QE system.

3. RESULTS AND DISCUSSION

In this paper, thioglycolic acid and ethanolamine were employed to dissolve elemental Cu, Zn, Sn, and Se powders. After stirring at 55 °C for several hours in air, we observed the disappearance of all elemental powders and the formation of a clear and homogeneous CZTSe precursor solution, as shown in the inset of Figure S2 in the Supporting Information. Note that the as-prepared CZTSe precursor solution has a relatively high viscosity of 4.35 Pa·S, which is not suitable for spin-coating. Thus, 2-methoxyethanol was used as the solvent to adjust the concentration and viscosity of CZTSe precursor solution before spin-coating process (~56 m Pa·S). Note that the CZTSe precursor solution is very stable in air and can be used to deposit CZTSe nanocrystal thin films without further purification. It was found that elemental Cu, Zn, Sn, and Se powders could not be dissolved in sole thioglycolic acid or ethanolamine. Additionally, we found that metallic Ga, In, Mg, Fe, Co, Ni, and Mn powders are also dissolved in thioglycolic acid and ethanolamine and the detailed dissolution mechanism will be investigated in our future work. The thermal decomposition behavior of CZTSe precursor solution was studied by thermal gravimetric analysis (TGA). TGA curve of the mixed CZTSe precursors with target ratios (Cu/(Zn + Sn) = 0.77 and Zn/Sn = 1.2) was shown in Figure S2 in the Supporting Information. The weight loss was found at 160−400 °C. Thereby, CZTSe nanocrystal thin films were fabricated by spin-coating CZTSe precursor solution, followed by sintering on a hot plate at 320 °C for 1 min. As can be seen in Figure 1, the crack-free CZTSe nanocrystal thin film with a thickness of 1.6 μm was obtained by repeating the spin-coating/sintering procedure. Finally, the large-grained CZTSe absorber layers were formed by selenization under Se atmosphere in a graphite box at 540 °C for 15 min.

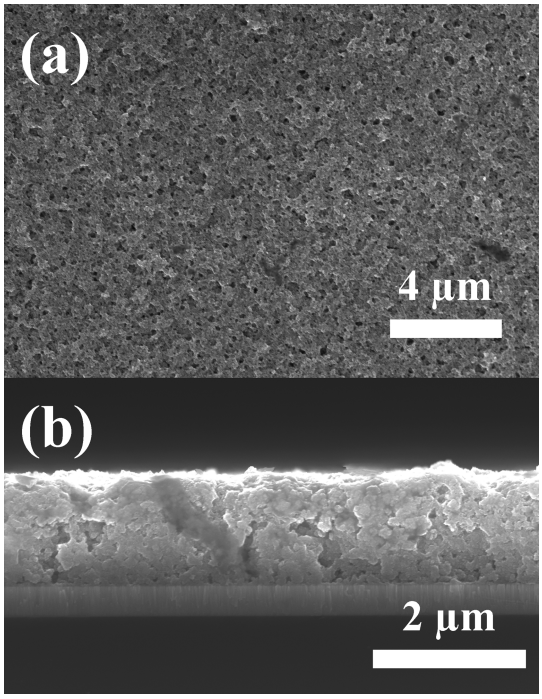

Figure 1. Top-view and cross-sectional SEM images of as-prepared CZTSe nanocrystal thin film: (a) top-view and (b) cross-sectional.

Figure 2a shows the X-ray diffraction (XRD) patterns of as-deposited and selenized CZTSe thin films. The three broad and weak XRD peaks were observed for as-prepared CZTSe thin films, which implies that as-prepared CZTSe thin films are composed of CZTSe nanoparticles with an average size of 8.0 nm calculated by Scherrer equation, confirming that CZTSe nanocrystal thin film can be directly fabricated by a simple molecular precursor-based solution approach without the need of complex nanocrystal synthesis. After the selenization, CZTSe thin films exhibit a standard kesterite structure (JCPDS No. 52−0868), and the intensity of the diffraction peaks increases, indicating the improvement of crystallinity and the increase of grain size, which are helpful for the high performance kesterite solar cells. Since the XRD patterns of some possible binary and ternary selenides, such as Cu_xSe, ZnSe, and Cu_2SnSe_3, are very analogous to that of CZTSe, the XRD pattern is insufficient to

dx.doi.org/10.1021/am5064926 | ACS Appl. Mater. Interfaces 2015, 7, 460−464

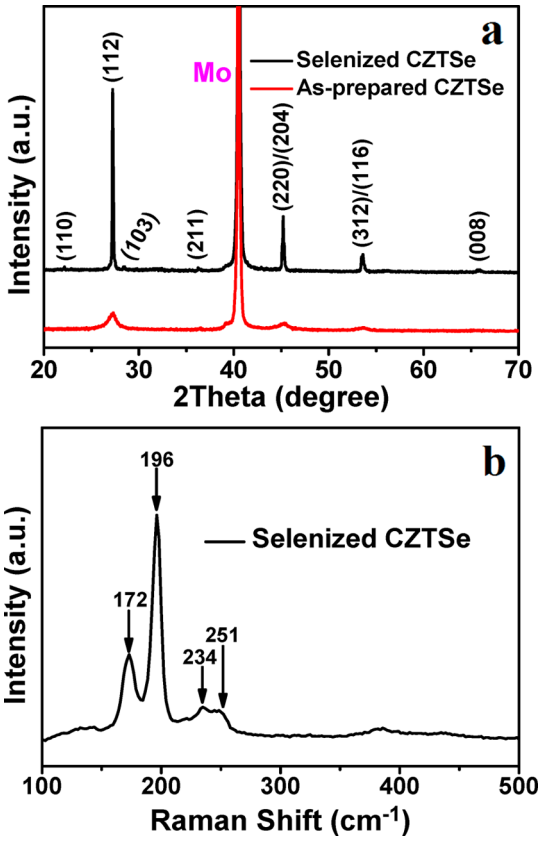

Figure 2. (a) XRD patterns of as-prepared CZTSe and selenized CZTSe thin films. (b) Raman spectrum of selenized CZTSe thin film.

identify the phase purity of CZTSe thin films. To detect these potential impurities, Raman spectrum of selenized CZTSe thin film was measured and is shown in Figure 2b. Three prominent Raman peaks located at 172, 196, and 234 cm^{-1} were observed, consistent with those reported values for kesterite CZTSe in the literature.[24] In addition, a weak peak at 251 cm^{-1} corresponding to binary ZnSe was observed. According to the previous reports, a small amount of ZnSe on the CZTSSe surface has no significant effect on the efficiency of kesterite solar cells.[16,25] Note that very harmful Cu_xSe and Cu_2SnSe_3 were not detected in the Raman spectrum of selenized CZTSe thin film.

Energy-dispersive X-ray spectroscopy (EDS) was employed to determine the chemical compositions of as-prepared and selenized CZTSe thin films (see Figure S3 in the Supporting Information). It has been demonstrated that Cu-poor and Zn-rich CZTSSe absorber layer is crucial to the high performance kesterite solar cells, and the optimum compositional ratio regions of Cu/(Zn+Sn) and Zn/Sn are 0.75−0.95 and 1.1−1.4, respectively.[11,26,27] In this work, CZTSe precursor solution with a target Cu/(Zn + Sn) ratio of 0.77 and Zn/Sn ratio of 1.2 was prepared. However, the ratios of Cu/(Zn + Sn) and Zn/Sn exhibit a slight increase for as-prepared CZTSe thin films (Cu/(Zn + Sn) = 0.91 and Zn/Sn = 1.25). After the selenization, both Cu/(Zn+Sn) and Zn/Sn ratios were almost unchanged, and the content of Se was increased from 47.68 to 49.41% (see Figure S3 in the Supporting Information). In addition, EDS analysis on the as-deposited CZTSe thin films revealed a small amount of sulfur (S/(S + Se) ≈ 0.07) resulting from undecomposed thioglycolic acid confirmed by TGA result. Interestingly, sulfur was not determined after the selenization, demonstrating the pure selenide CZTSe thin films were formed. To identify the valence states of four types of elements in the CZTSe thin films, we measured X-ray photoelectron spectroscopy (XPS) (see Figure S4 in the Supporting Information). The Cu 2p peaks located at 931.6 and 951.7 eV with a splitting value of 20.1 eV (seeFigure S4a in the Supporting Information), correspond to Cu^+ ions. The Zn 2p shows two peaks at 1021.4 and 1044.2 eV (see Figure S4b in the Supporting Information), which is consistent with the standard peak separation for Zn^{2+}. The Sn 3d spectrum is representative of Sn^{4+} (see Figure S4c in the Supporting Information). The Se 3d peak (see Figure S4d in the Supporting Information) shows the characteristic of Se^{2-}.[28] These XPS data demonstrated that $Cu_2ZnSnSe_4$ is formed.

It has been reported that the morphology and crystal size of the absorber layer are crucial for the performance of the kesterite solar cells.[29] The morphologies of the selenized CZTSe thin films under different selenization conditions were shown in Figure S5 in the Supporting Information. It was observed that the surface morphology of the CZTSe thin film selenized at 530 °C for 15 min is the best, which is very dense and has only few bright spots on the surface, but the best PCE was achieved for CZTSe thin film selenized at 540 °C for 15 min. Thus, this selenization condition is regarded as the optimal selenization condition. Figure 3a shows high-resolution top-view SEM image of the selenized CZTSe thin film under the optimal selenization condition. Large-grained and densely packed CZTSe thin film with grain size of 1−2 μm was achieved after the selenization. Furthermore, some bright spots on the surface were observed, and they should be high resistance ZnSe, which is consistent with the observation of Raman spectrum. Figure 3b shows a cross-sectional SEM image of a completed CZTSe solar cell device. The selenized CZTSe thin film consists of the large-grain layer and the fine-grain layer. The thickness of the large-grain layer is ~1.0 μm, which can meet the requirements for the highly efficient kesterite solar

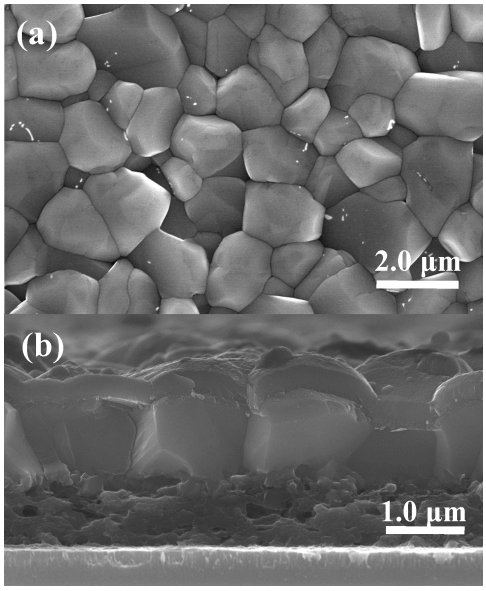

Figure 3. (a) High-resolution top-view SEM image of selenized CZTSe thin film under the optimal selenization condition. (b) Cross-sectional SEM image of a completed glass/Mo/CZTSe/CdS/i-ZnO/ITO/Al solar cell device.

dx.doi.org/10.1021/am5064926 | ACS Appl. Mater. Interfaces 2015, 7, 460−464

cells. Also, a ~850 nm thick carbon-rich fine-grain CZTSe layer is formed nearby Mo electrode. Figure S6 in the Supporting Information shows the cross-sectional SEM and EDS line scans using SEM mode of the as-prepared CZTSe thin film. The as-prepared CZTSe thin film contains large amounts of carbon, which reveals the carbon contained in fine-grain layer is probably associated with the thermal decomposition of the viscous CZTSe precursor solution. According to the reports for high-performance CZTSSe solar cells fabricated by a solution-based approach, the carbon-rich fine-grain CZTSe layer seems to have no significant effect on the performance of the CZTSSe solar cells.[10,12]

The dark and light $J-V$ curves of the best CZTSe solar cell are shown in Figure 4a. Under simulated solar light illumination

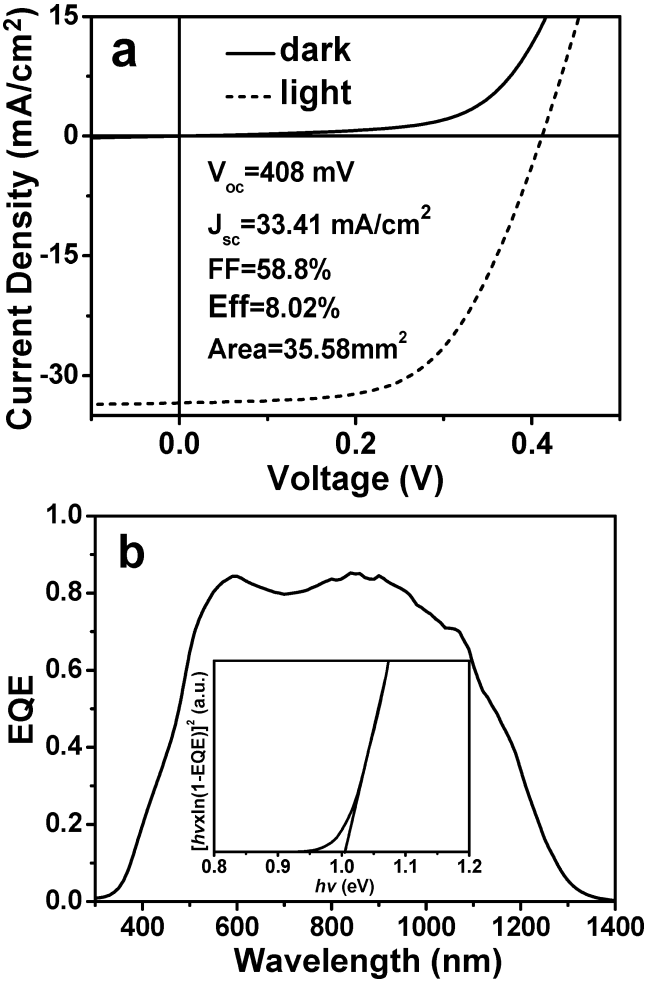

Figure 4. (a) $J-V$ curves of the best CZTSe solar cell in the dark and under air mass (AM) 1.5 illumination. (b) EQE spectrum of the corresponding device; inset: the band gap of corresponding device was determined to be ~1.00 eV by plotting $[E\ln(1 - \mathrm{EQE})]^2$ vs E.

(AM1.5), the best device yielded a PCE of 8.02% with short circuit current density (J_{sc}) of 33.4 mA cm^{-2}, open circuit voltage (V_{OC}) of 408 mV, and fill factor (FF) of 0.588. The PCEs of other devices fabricated under different conditions are 7–8% (see Table S1 in the Supporting Information). The top ten CZTSe solar cells have an average PCE of 7.69%. Note that our J_{sc} is somewhat lower than 38.9 mA cm^{-2} of the best CZTSe solar cell in the literature,[15] which may be due to the lack of antireflection coating. Figure 4b presents the external quantum efficiency (EQE) spectrum of the corresponding solar cell, and the EQE curve shows a strong response of above 80% in the wavelength range of 540 to 960 nm, indicating a wide depletion region and the super collection efficiency due to slight recombination losses. The calculated J_{sc} from the EQE spectrum is 33.8 mA cm^{-2}, which is very close to the measured value from the light $J-V$ curve. The inset of Figure 4b shows the band gap of CZTSe thin film by plotting $[E\ln(1 - \mathrm{EQE})]^2$ vs E, which was determined to be ~1.00 eV, same as E_g in the literature.[30] The shunt resistance (R_{sh}), the series resistance (R_s), and the diode quality factor (A) of the CZTSe solar cell are 435 Ω cm^2, 1.5 Ω cm^2, and 1.7, respectively, which were obtained by the standard dark $J-V$ curve analysis (see Figure S7 in the Supporting Information).

4. CONCLUSIONS

In summary, we developed a novel precursor-based solution approach to fabricate high quality CZTSe thin films. The elemental Cu, Zn, Sn, and Se powders were simultaneously dissolved in the mixed thiol/amine solution, forming the homogeneous CZTSe precursor solution at molecular level, and this is the first report on the simultaneous dissolution of elemental Cu, Zn, Sn, and Se powders. Through this solution-based approach, the selenized CZTSe thin films are extremely dense and compact. A PCE of 8.02% has been realized for CZTSe thin film solar cells. More interestingly, other metallic powders, such as Ga, In, Mg, Fe, Co, Ni, Mn, etc., can also be dissolved by this approach, providing a general and environmental friendly solution approach to prepare many types of metal–organic precursor solutions and fabricate a variety of metal chalcogenide thin films. In the future work, we will focus on understanding the dissolution mechanism of metal powders in the thiol/amine solution and further improving the photoelectric conversion efficiency of CZTSe solar cells.

■ ASSOCIATED CONTENT

Supporting Information

Digital photographs of the dissolution of elemental Cu, Zn, and Sn powders; TGA curve; XPS and EDS spectra; cross-sectional SEM and EDS line scans of the as-prepared CZTSe thin film; SEM of selenized CZTSe thin film under different selenization conditions; PCEs of the devices under different conditions; analysis of light and dark $J-V$ curves. This material is available free of charge via the Internet at http://pubs.acs.org.

■ AUTHOR INFORMATION

Corresponding Author

*E-mail: pan@ciac.ac.cn.

Notes

The authors declare no competing financial interest.

■ ACKNOWLEDGMENTS

This work was supported by National Natural Science Foundation of China (Grants 1333108, 51302258, 51172229, and 51202241).

■ REFERENCES

(1) Jackson, P.; Hariskos, D.; Lotter, E.; Paetel, S.; Wuerz, R.; Menner, R.; Wischmann, W.; Powalla, M. New World Record Efficiency for Cu(In,Ga)Se_2 Thin-Film Solar Cells beyond 20%. *Prog. Photovolt: Res. Appl.* **2011**, *19*, 894–897.

(2) Wang, K.; Gunawan, O.; Todorov, T.; Shin, B.; Chey, S. J.; Bojarczuk, N. A. Structural and Elemental Characterization of High Efficiency Solar Cells. *Appl. Phys. Lett.* **2011**, *98*, 051912.
(3) Todorov, T. K.; Tang, J.; Bag, S.; Gunawan, O.; Gokmen, T.; Zhu, Y.; Mitzi, D. B. Beyond 11% Efficiency: Characteristics of State-of-the-Art $Cu_2ZnSn(S,Se)_4$ Solar Cells. *Adv. Energy Mater.* **2013**, *3*, 34−38.
(4) Bag, S.; Gunawan, O.; Gokmen, T.; Zhu, Y.; Todorov, T. K.; Mitzi, D. B. Low Band Gap Liquid-Processed CZTSe Solar Cell with 10.1% Efficiency. *Energy Environ. Sci.* **2012**, *5*, 7060−7065.
(5) Winkler, M. T.; Wang, W.; Gunawan, O.; Hovel, H. J.; Todorov, T.; Mitzi, D. B. Optical Designs that Improve the Efficiency of $Cu_2ZnSn(S,Se)_4$ Solar Cells. *Energy Environ. Sci.* **2014**, *7*, 1029−1036.
(6) Yang, W.; Duan, H. S.; Bod, B.; Zhou, H.; Lei, B.; Chung, C. H.; Li, S. H.; Hou, W. W.; Yang, Y. Novel Solution Processing of High-Efficiency Earth-Abundant $Cu_2ZnSn(S,Se)_4$ Solar Cells. *Adv. Mater.* **2012**, *24*, 6323−6329.
(7) Barkhouse, D.; Gunawan, O.; Gokmen, T.; Todorov, T. K.; Mitzi, D. B. Device Characteristics of a 10.1% Hydrazine-Processed $Cu_2ZnSn(Se,S)_4$ Solar Cell. *Prog. Photovolt: Res. Appl.* **2012**, *20*, 6−11.
(8) Wang, W.; Winkler, M. T.; Gunawan, O.; Gokmen, T.; Todorov, T. K.; Zhu, Y.; Mitzi, D. B. Device Characteristics of CZTSSe Thin-Film Solar Cells with 12.6% Efficiency. *Adv. Energy Mater.* **2014**, *4*, 1301465.
(9) Hsu, W. C.; Bod, B.; Yang, W.; Chung, C. H.; Yang, Y. Reaction Pathways for the Formation of $Cu_2ZnSn(Se,S)_4$ Absorber Materials from Liquid-Phase Hydrazine-Based Precursor Inks. *Energy Environ. Sci.* **2012**, *5*, 8564−8571.
(10) Miskin, C. K.; Yang, W. C.; Hages, C. J.; Carter, N. J.; Joglekar, C. S.; Stach, E. A.; Agrawal, R. 9.0% Efficient $Cu_2ZnSn(S,Se)_4$ Solar Cells from Selenized Nanoparticle Inks, *Prog. Photovolt: Res. Appl.* **2014**, DOI: 10.1002/pip.2472.
(11) Leidholm, C.; Hotz, C.; Breeze, A.; Sunderland, C.; Ki, W. Final Report: Sintered CZTS Nanoparticle Solar Cells on Metal Foil. *NREL Subconstract Report* **2012**, NREL/SR-5200−56510.
(12) Cao, Y.; M. S, D., Jr.; Caspar, J. V.; Farneth, W. E.; Guo, Q.; Ionkin, A. S.; Johnson, L. K.; Lu, M.; Malajovich, I.; Radu, D.; Rosenfeld, H. D.; Choudhury, K. R.; Wu, W. High-Efficiency Solution-Processed $Cu_2ZnSn(S,Se)_4$ Thin-Film Solar Cells Prepared from Binary and Ternary Nanoparticles. *J. Am. Chem. Soc.* **2012**, *134*, 15644−15647.
(13) Schnabel, T.; Löw, M.; Ahlswede, E. Vacuum-Free Preparation of 7.5% Efficient $Cu_2ZnSn(S,Se)_4$ Solar Cells Based on Metal Salt Precursors. *Sol. Energy Mater. Sol. Cells* **2013**, *117*, 324−328.
(14) Repins, I.; Beall, C.; Vora, N.; DeHart, C.; Kuciaukas, D.; Dippo, P.; To, B.; Mann, J.; Hus, W. C.; Goodrich, A.; Noufi, R. Co-Evaporated $Cu_2ZnSnSe_4$ Films and Devices. *Sol. Energy Mater. Sol. Cells* **2012**, *101*, 154−159.
(15) Brammertz, G.; Buffière, M.; Oueslati, S.; ElAnzeery, H.; Messaoud, K. B.; Sahayaraj, S.; Köble, C.; Meuris, M.; Poortmans, J. Characterization of Defects in 9.7% Efficient $Cu_2ZnSnSe_4$-CdS-ZnO Solar Cells. *Appl. Phys. Lett.* **2013**, *103*, 163904.
(16) Hsu, W. C.; Repins, I.; Beall, C.; DeHart, C.; Teeter, G.; To, B.; Yang, W.; Yang, Y.; Noufi, R. Growth Mechanisms of Co-Evaporated Kesterite: a Comparison of Cu-Rich and Zn-Rich Composition Paths. *Prog. Photovolt: Res. Appl.* **2014**, *22*, 35−43.
(17) Jeon, J. O.; Lee, K. D.; Oh, L. S.; Seo, S. W.; Lee, D. K.; Kim, H.; Jeong, J. H.; Ko, M. J.; Kim, B. S.; Son, H. J.; Kim, J. Y. Highly Efficient Copper-Zinc-Tin-Selenide (CZTSe) Solar Cells by Electrodeposition. *ChemSusChem* **2014**, *7*, 1073−1077.
(18) Webber, D. H.; Brutchey, R. L. Alkahest for V_2VI_3 Chalcogenides: Dissolution of Nine Bulk Semiconductors in a Diamine-Dithiol Solvent Mixture. *J. Am. Chem. Soc.* **2013**, *135*, 15722−15725.
(19) Liu, Y.; Yao, D.; Shen, L.; Zhang, H.; Zhang, X.; Yang, B. Alkylthiol-Enabled Se Powder Dissolution in Oleylamine at Room Temperature for the Phosphine-Free Synthesis of Copper-Based Quaternary Selenide Nanocrystals. *J. Am. Chem. Soc.* **2012**, *134*, 7207−7210.
(20) Johnson, M.; Baryshev, S. V.; Thimsen, E.; Manno, M.; Zhang, X.; Veryovkin, I. V.; Leighton, C.; Aydil, E. S. Alkali-Metal-Enhanced Grain Growth in Cu_2ZnSnS_4 Thin Films. *Energy Environ. Sci.* **2014**, *7*, 1931−1938.
(21) Zhao, W. G.; Cui, Y.; Pan, D. C. Air-Stable, Low-Toxicity Precursors for $CuIn(SeS)_2$ Solar Cells with 10.1% Efficiency. *Energy Technol.* **2013**, *1*, 131−134.
(22) Wang, G.; Wang, S. Y.; Cui, Y.; Pan, D. C. A Novel and Versatile Strategy to Prepare Metal-Organic Molecular Precursor Solutions and Its Application in $Cu(In,Ga)(S,Se)_2$ Solar Cells. *Chem. Mater.* **2012**, *24*, 3993−3997.
(23) Tian, Q. W.; Wang, G.; Zhao, W. G.; Chen, Y. Y.; Yang, Y. C.; Huang, L. J.; Pan, D. C. Versatile and Low-Toxic Solution Approach to Binary, Ternary, and Quaternary Metal Sulfide Thin Films and Its Application in $Cu_2ZnSn(S,Se)_4$ Solar Cells. *Chem. Mater.* **2014**, *26*, 3098−3103.
(24) Redinger, A.; Hönes, K.; Fontané, X.; Roca, V. I.; Saucedo, E.; Valle, N.; Rodríguez, A.; Siebentritt, S. Detection of a ZnSe Secondary Phase in Coevaporated $Cu_2ZnSnSe_4$ Thin Films. *Appl. Phys. Lett.* **2011**, *98*, 101907.
(25) Hsu, W. C.; Repins, I.; Beall, C.; DeHart, C.; Teeter, G.; To, B.; Yang, Y. The Effect of Zn Excess on Kesterite Solar Cells. *Sol. Energy Mater. Sol. Cells* **2013**, *113*, 160−164.
(26) Wang, G.; Zhao, W. G.; Cui, Y.; Tian, Q. W.; Gao, S.; Huang, L. J.; Pan, D. C. Fabrication of a $Cu_2ZnSn(S,Se)_4$ Photovoltaic Device by a Low-Toxicity Ethanol Solution Process. *ACS Appl. Mater. Interfaces* **2013**, *5*, 10042−10047.
(27) Katagiri, H.; Jimbo, K.; Maw, W. S.; Oishi, K.; Yamazaki, M.; Araki, H.; Takeuchi, A. Development of CZTS-Based Thin Film Solar Cells. *Thin Solid Films* **2009**, *517*, 2455−2460.
(28) Shavel, A.; Arbiol, J.; Cabort, A. Synthesis of Quaternary Chalcogenide Nanocrystals: Stannite $Cu_2Zn_xSn_ySe_{1+x+2y}$. *J. Am. Chem. Soc.* **2010**, *132*, 4514−4515.
(29) Zhou, H.; Hsu, W. C.; Duan, H. S.; Bob, B.; Yang, W.; Song, T. B.; Hsu, C. J.; Yang, Y. CZTS Nanocrystals: a Promising Approach for Next Generation Thin Film Photovoltaics. *Energy Environ. Sci.* **2013**, *6*, 2822−2838.
(30) Shin, B.; Zhu, Y.; Bojarczuk, N. A.; Chey, S. J.; Guha, S. Control of an Interfacial $MoSe_2$ Layer in $Cu_2ZnSnSe_4$ Thin Film Solar Cells: 8.9% Power Conversion Efficiency with a TiN Diffusion Barrier. *Appl. Phys. Lett.* **2012**, *101*, 053903.